INFLUENCE MECHANISM OF THICKNESS AND VISCOSITY OF FLAT ENERGY DIRECTOR TO THE JOINTS QUALITY BY ULTRASONIC WELDING

Jiale Lu[1], Wei Dai[2], Jun Wang[2,3], Xianghui Gan, Zhuang Wu, Hang Wang, Xujun Tian[4]

[1]Princeton International School of Mathematics and Science, Princeton 08540, NJ, USA
[2]School of Materials Science and Engineering, Wuhan University of Technology, Wuhan 430070, PR China
[3]Institute of Advanced Material Manufacturing Equipment and Technology, Wuhan University of Technology, 430070, Wuhan, China
[4]China Ship Development and Design Center, Wuhan 430064, China

ABSTRACT

The research in this paper is an essential part of a bigger effort to develop ultrasonic welding using flat energy directors (FED) in thermoplastic composites. It mainly focused on assessing the effect of the changes in thickness and viscosity of FED on welding strength and welding strength stability. Furthermore, the welding and failure mechanisms were investigated by monitoring the real-time temperature evolution at the interface and analyzing the welding area (WA) and the macro and microfracture surface. From the experimental results, the use of FED with thinner thickness (0.1-0.2 mm) and slightly higher viscosity greatly improved weld strength and weld strength stability. Due to the effect of glass fibers forming a mechanical interlocking effect between the adherend and FED, joints with 20% SGF/PP FED also had a surprisingly excellent weld quality. Welding area analysis indicated a significantly positive correlation between the lap shear strength I and the welded area for the joints with FED. Based on real-time temperature curves, thinner FED had an improvement on the initial temperature rate and the most temperature curves leveled off at the onset melting temperature (Tonset) of the FED after a time-lapse of about 0.4 s. Morphology analysis showed that the melting and flow of matrix at the interface started at the edges of the overlap; the melting area and morphology of the interfaces with 1% EG/PP FED and 20% SGF/PP are much bigger and coarse. And failure mechanisms of the joints with FED are a combination of adhesive failure, cohesive failure, and fiber-matrix debonding failure.

KEYWORDS

Ultrasonic welding, thermoplastic, joint quality, flat energy director, thickness and viscosity.

1. INTRODUCTION

As a result of short welding times, good welding quality and ease of automation, ultrasonic welding of thermoplastic composites is a very attractive assembling technique [1-4]. From a mechanical point of view, it allows joints to have high static properties, low through-thickness porosity, and lower weight compared to fastened counterparts [5]. The ultrasonic welding of thermoplastics is based on low-amplitude (2.5–250 μm peak-to-peak amplitude) and high-frequency (20–40 kHz) vibrations that cause surface friction and viscoelastic heating at the welding interface [5]. Conventionally, the energy directors are employed in ultrasonic welding to

concentrate the heat and increase the heat transfer in the contacting surface [6,7]. Additionally, it has been proven that ED plays an important role in realizing stable welding quality [8]. However, the utilization of triangular ridges molded on the substrate would limit the freedom of the design while complicating the manufacturing process of parts. The extensive optimization of the shape, size, number, and orientation of the energy directors will also extend the time and cost from design to manufacturing. To avoid using special forms of ED, some researchers used a loose matrix resin film, also known as "flat energy director (FED)," as a new kind of ED [9,10,21]. I.F Villegas assessed whether the simplicity in manufacturing offered by the flat energy directors has any counteracting effect in the welding process. Analysis of welding energy and time, as well as weld strength compared to more traditional energy directing solutions, showed that flat energy directors, which significantly simplify ultrasonic welding of thermoplastic composites, do not have any substantial negative impact on the welding process or the quality of the welded joints [11]. I.F Villegas further studied the relationship between weld strength and the welding process data, namely dissipated power and displacement of the sonotrode, in ultrasonic welding of thermoplastic composite parts with flat energy directors. The results showed that the relationship, combined with displacement-controlled welding, allows for the fast definition of optimum welding parameters that consistently result in high-strength welded joints [12]. Also, the effect of the thickness of flat energy directors (ED) on heat generation at the interface was investigated by Genevieve Palardy and Irene Fernandez Villegas [13]. Power and displacement data showed clear differences caused by the change of thickness, related to heat concentration at the weld line during the welding process. Successful welds obtained with flat energy directors consisting of a loose matrix resin film placed at the welding interface were mostly related to the rapid melting behaviors of the flat energy director as a result of the lower compressive stiffness of the resin film as compared to the stiffness of the composite adherends.

To gain full advantage of joining thermoplastics using flat energy directors, it is vital to understand the mechanisms of welding. The existing literature concerning the mechanisms of ultrasonic welding using flat energy directors is rather disparate and scarce [14-18]. The influence mechanism of processing parameter to the joint using flat energy directors was investigated by monitoring the real-time temperature at interfaces in Wang's laboratory. They found that the heating rate can be accelerated by using FED and that the peak temperature was lowered. When the vibration time reached 0.9s, the interfacial bonding was sound and the FED was completely melted. The thermal stress between carbon fiber and resin was reduced, and the weld strength peaked with the highest value of 28 MPa [15]. In addition, Ramarathnam G examined the melting process and failure mode of the welding interface with FED of different MFI (Melting Flow Index) by recording the welding process using a high-speed camera and by observing the morphology of the heat-affected-zone [19]. A numerical model was used by Arthur Levy to investigate the physical mechanisms and the heating phenomena of ultrasonic welding with flat energy directors. The results showed that the first heating mechanism is confirmed to be the result of interfacial friction. Bulk viscoelastic dissipation becomes predominant when the interface reaches higher temperatures. The dissipated power is suddenly increased when the whole interface reaches the glass transition temperature [10]. Hence, on the basis of previous experimental results, more systematic and stringent studies are indispensable for the explicit understanding of the ultrasonic welding mechanisms with flat energy directors.

The primary focus of the present study is the relationships between the properties of flat energy director and weld quality. Specifically, the research addresses the effect of the thickness and viscosity of flat energy director on the lap shear strength of ultrasonic welded Polypropylene (PP). In order to fully understand and quantify the phenomena taking place in the flat-energy-director ultrasonic welding process, the temperature developed at the welding interface and the extension of the heat-affected zone (HAZ) in the adherends were investigated by real-time temperature monitoring and morphology observation of the fracture surface. This work is

instrumental for understanding the joint formation mechanism and the mode of failure by ultrasonic welding with flat energy directors, both of which will allow the welding process to be further optimized.

2. EXPERIMENTAL

2.1. Adherends

The adherends used in this study were polypropylene (PP-S1003) with melt flow index 3 g/10 min supplied by Shanghai SECCO Petrochemical Co. LTD. The adherends were formed by a table-top press forming machine R-3201 (Wuhan Qi'en Technology Co., Ltd. China) with a press condition of 200°C and 20 MPa for 15 min. The adherends used all had dimensions of 100×15×4mm, as shown in Fig. 1a.

Flat energy director (FED) made of four different materials (Pure PP, 1% EG/PP, 3% MWNT/PP, 20% SGF/PP) were used in this study to improve the welding quality of the joints. These four materials were prepared by an internal mixer that rotates at 60r/min at 190℃ for 15mins. The viscosity of the four materials has been measured by a rheometer (MCR 102, Anton Paar), as shown in Fig. 2b. The sort of size of low shear rate viscosity values of these four materials is: Pure PP < 1% EG/PP < 3% MWNT/PP < 20% SGF/PP. The differential scanning calorimeter (DSC) analysis results of the four flat energy directors were shown in Fig. 1c. For each material, flat energy director with the thickness of 0.1mm, 0.2mm, and 0.3mm were tested, each with 6 trials. These trials form the basis for later comparisons to the mechanical result. Two types of joints (with and without FED) were welded to clarify the effect of FED.

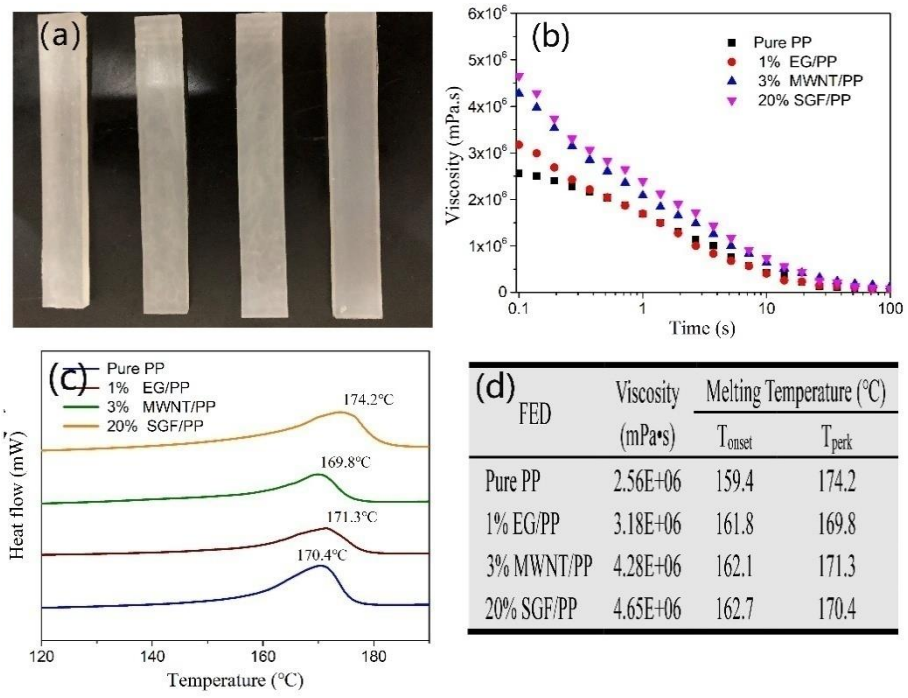

(d)

FED	Viscosity (mPa•s)	Melting Temperature (℃) T_{onset}	T_{perk}
Pure PP	2.56E+06	159.4	174.2
1% EG/PP	3.18E+06	161.8	169.8
3% MWNT/PP	4.28E+06	162.1	171.3
20% SGF/PP	4.65E+06	162.7	170.4

Figure 1. (a) Welding samples made of PP. (b) Viscosity curves of flat energy director. (c) DSC analysis of flat energy director. (d) The data of viscosity at the low shear rate and melting temperature of flat energy director.

2.2. Ultrasonic Welding Process

The ultrasonic welding process was performed using a Model YX-1535 multifunction ultrasonic welding (UW) machine produced by Dongwan Yixin Automation Equipment Co., Ltd with a frequency of 20 kHz and a power of 1.0 kW.

Fig. 2a-b shows the schematic illustration of the ultrasonic welding process using flat energy directors, the welding set-up equipped with a rectangular sonotrode and a temperature data collection system. The flat energy director was placed between the top and bottom adherends and was clamped using an aluminum fixture. Unless otherwise stated, the standard operating conditions involved the following parameter settings: an applied pressure of 2 MPa, a welding time of 1.5s, a pressure holding time of 4s and an amplitude of 50 μm.

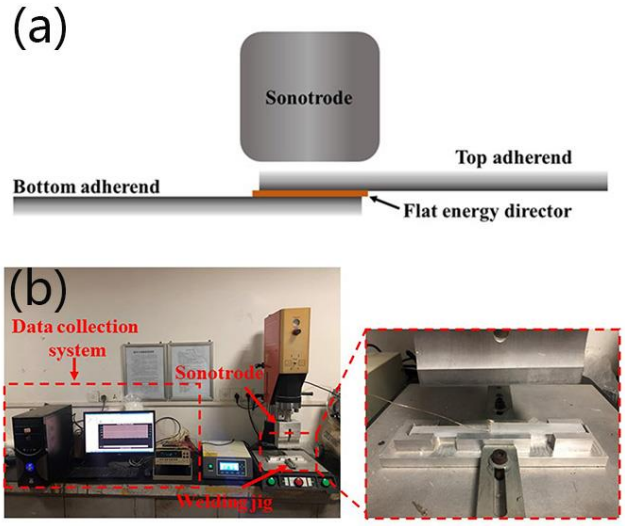

Figure 2 (a) Schematic illustration of the ultrasonic welding process using flat energy directors. (b) Ultrasonic welding device and temperature data collection system used in this study.

2.3. Testing and Characterization

According to the national shear strength testing standard of HG/T 4281-2011, the lap shear strength of the single-lap welded sample was mechanically tested in a microcomputer control electron universal testing machine (Shenzhen Reger Instrument Co., Ltd. China Model RG100-10) with a tensile velocity of 2 mm/min. In order to make sure that, in the mechanical test, the two forces exerted on the two ends of the product would not produce any extra torque at the interface, both ends of the specimens were welded with extra pieces that had the same thickness as the adherends, as shown in Fig. 3a. The lap shear strength (LSS) was calculated in two ways as proposed by Goto et al [20]. LSS Ⅰ is calculated as the maximum load divided by the entire overlap area, i.e. 15×12.5 mm2, while LSS Ⅱ is calculated as that result divided by the actual welded area. LSS Ⅰ and LSS Ⅱ are the indicators for “welding efficiency” and “welding quality,” respectively. Fig.3b shows the schematic illustration of the lap shear test. The actual welded area was obtained from fractured surface observations of the joints after the tests. As shown in the Fig.3c, the actual welding area was measured by an application called ImageJ.

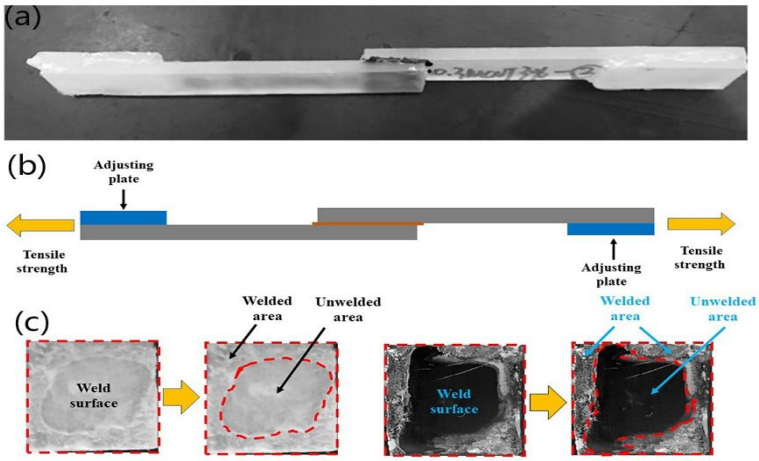

Figure 3 (a) Lap shear test sample with flat energy directors. (b) Schematic illustration of lap shear test with flat energy director. (c) The representative fracture surface of the joint with flat energy director and the corresponding welded area (WA).

To get a better understanding of the properties of flat energy director on the lap shear strength and the formation mechanism of the joints, the temperature evolutions at the interface were monitored. As shown in the Fig.2b, the experimental setup for temperature measurements consists of a data collection system and a K-type thermocouple, containing two entwined wires, each with a diameter of 0.125mm, which was placed in the welding interface. During the ultrasonic welding process, the real-time temperature monitoring was recorded as a function of time by a data collection system (Keithley 2700).

After the mechanical test, the fracture interface was used to assess the changes at the welding interface in the different welding conditions by using a high-resolution Gaosuo Digital Microscope. Further fracture analysis was carried out on welded specimens with a JEM-7500F Scanning Electron Microscope (SEM) to evaluate the failure modes in the different welding conditions.

3. EXPERIMENTAL RESULTS AND DISCUSSION

3.1. The Effect of Thickness and Viscosity of Flat Energy Director on the Lap Shear Strength.

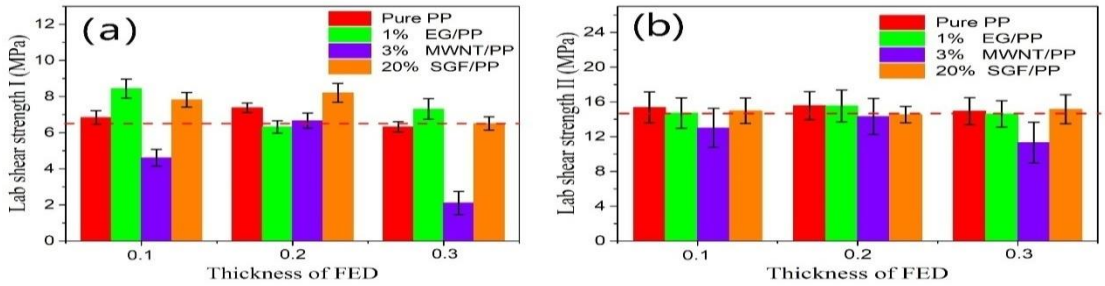

Figure 4 (a) Lap shear strength Ⅰ (LSS Ⅰ) for the joints with different flat energy directors (FED). (b) Lap shear strength Ⅱ (LSS Ⅱ) for the joints with different flat energy directors (FED). Note that the sort of size of low shear rate viscosity values of these four materials is: Pure PP < 1% EG/PP < 3% MWNT/PP < 20% SGF/PP. The red dash line in Fig. 4a-b represents the average lap shear strength of PP without FED.

Fig. 4(a) shows lap shear strength I (LSS Ⅰ) for the joints with different flat energy directors (FED). LSS Ⅰ is calculated as the maximum load divided by the entire overlap area. As Fig. 4a reveals, LSS Ⅰ of the joints with FED welded at a thickness of 0.2 mm achieved the highest value, except the 1% EG/PP FED, which achieved the maximum at a thickness of 0.1 mm. The lowest LSS Ⅰ of the joints with FED welded was achieved at a thickness of 0.3 mm, except the 1% EG/PP FED, which achieved the minimal at a thickness of 0.2 mm. Therefore, it is reasonable to deduce that when the thickness of flat energy directors ranges from 0.1 mm to 0.2 mm, the joints achieve excellent weld strength. In addition, it can be found that, at some specific thickness, LSS Ⅰ of the joints added with these four different FED exceeded LSS I of the joints without FED. In particular, LSS Ⅰ of the joint added with 0.1 mm 1% EG/PP FED reached the highest value of 8.44 MPa, a 29.4% improvement over LSS I of the joints without FED, as shown in Table 1. From table 1, we can still find that the scatters of LSS Ⅰ for the joints with FED are less than that for the joints without FED. From the previous analysis, we can conclude that the use of flat energy directors effectively improves the joints in two ways: weld strength and weld strength stability.

In addition to the thickness of the flat energy directors, the fluidity of flat energy directors, namely the viscosity, has a great effect on the weld strength. Compared to the joints welded with 1% EG/PP FED, which have a viscosity of 3.18×106 mPa•s, almost 1.3 times bigger than that of pure pp, the LSS Ⅰ of the joints with pure pp FED is smaller than it is under the condition of same FED thickness. However, compared to joints welded with 3%MWNT/PP FED, which have a viscosity of 4.28×106 mPa•s, almost 1.7 times bigger than that of pure pp, the LSS I of the joints with pure pp FED is much bigger than it is under the condition of same FED thickness. Therefore, the experimental results reinforce our prediction that viscosity great effects weld strength. Furthermore, when the viscosity of FED is slightly bigger than the base material, a better weld strength will be achieved. However, there is a surprising phenomenon that LSS I of the joints added with 20% SGF/PP, which have a slightly bigger viscosity than 3%MWNT/PP, are much bigger than that of the joints welded with 3%MWNT/PP. The answer to this phenomenon will be discussed in the following chapters in detail.

Lap shear strength Ⅱ (LSS Ⅱ) for the joints with different flat energy directors (FED) is shown in Fig. 4b. LSS Ⅱ is calculated as that divided by the actual welded area, which is the indicator for “welding quality”. It can be found in Fig. 4b that LSS Ⅱ of the joints with 3% MWNT/PP FED was still low. The rest joints have good welding quality, which is slightly stronger than the joints without FED. This means that compared to the parameter of the thickness of FED, the viscosity of FED contributes more substantially to welding quality. In terms of LSS I and LSS Ⅱ, it can be confirmed that the efficiency and quality of the joints welded with FED, except for 3% MWNT/PP FED, are almost the same. Although the welding quality of the joints with FED appears to be larger than that of the joints without FED, the joint quality seems to be insufficient in comparison with the tensile strength of adherend, e.g. 35 MPa. Here, the scatters of LSS Ⅱ for the joints with FED are larger than the scatters of LSS I for the joints with FED. This is because that the scatters of LSS2 include the scatters of the maximum load and the welded area, while those of LSS1 are affected by only the maximum load. The mechanism of these different welding efficiencies and quality for these joints was investigated in the next subsection.

Table 1. Lap shear strength I (LSS I) for the joints with different flat energy directors (FED).

Thickness of FED	Lab shear strength I (MPa) with different material of FED				
	No FED	Pure PP	1% EG/PP	3% MWNT/PP	20% SGF/PP
No FED	6.52±0.47	-	-	-	-
0.1 mm	-	6.84±0.38	8.44±0.53	4.61±0.47	7.82 ± 0.41
0.2 mm	-	7.38±0.26	6.32±0.34	6.67±0.42	8.21± 0.52
0.3 mm	-	6.32±0.28	7.31±0.57	2.11 ± 0.64	6.51± 0.37

3.2. The Effect of Thickness and Viscosity of Flat Energy Director on the Welded Area.

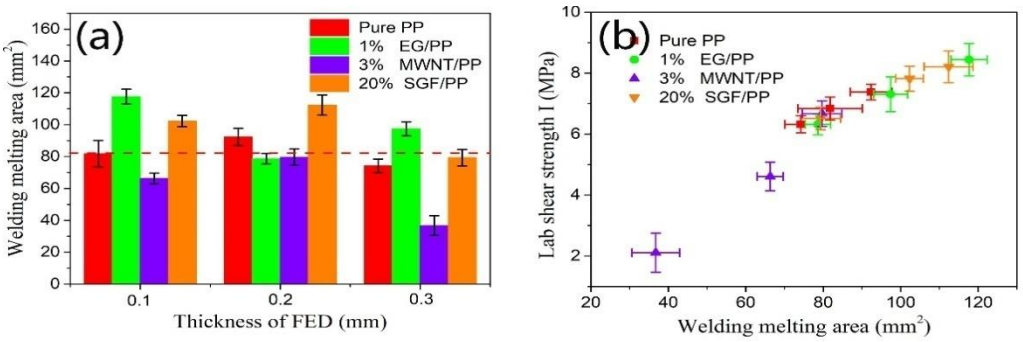

Fig. 5 (a) Welded area of the joints with different flat energy directors (FED). (b) Lap shear strength I (LSS I) versus welded area for the joints welded with different flat energy directors (FED). Note that the red dash line in Fig. 5a represents the average welded area of the joints without FED.

Fig. 5a shows the welded area of the joints with different flat energy directors (FED). As Fig. 3a reveals, the welded area of the joints with 0.3 mm FED is lower than that of the joints welded with 0.1 mm and 0.2 mm FED, which has a good agreement with the LSS I. In addition, at some specific thickness, the welded area of the joints added with FED except 3%MWNT/PP FED exceeded the welded area of the joints without FED. In particular, the welded area of the joint added with 0.1 mm 1% EG/PP FED reached the highest value of 117.64 mm2, a 42.97% improvement over the welded area of the joints without FED, as shown in Table 2. Thus, these results, as shown in Fig.3a and Table 2, indicate that the use of a flat energy director has an effective improvement in the welded area. Furthermore, there is a significant positive correlation between the lap shear strength Ⅰ (LSS Ⅰ) and the welded area of the joints added with FED, as shown in Fig. 3b. However, the exact mathematical relationship between them is very complicated and is not shown in this article. More research is needed in this area to determine the precise relation. Here, the scatters of the welded area for the joints with FED are large than that for the joints without FED, which perfectly explains the reason for the larger scatters of the LSS 2.

From the point of view of the viscosity of FED, the relationship between the welding area and the viscosity of FED coincides with the relationship between LSS Ⅰ and the viscosity of FED. The welding area of the joints with 1% EG/PP FED that has a slightly bigger viscosity is bigger than that of added with pure pp FED. And the joints welded with 3%MWNT/PP FED have a smaller welding area than that of welded with pure pp FED. Moreover, the surprising

phenomenon mentioned concerning LSS 1 between the joints with 3%MWNT/PP FED and the joints with 20% SGF/PP FED also occurred in the relationship between welding area and viscosity. The joints welded with 20% SGF/PP FED have a bigger welding area than the joints with 3%MWNT/PP FED, which has a smaller viscosity than the former. It is worth pointing out that, when the welding area was greater than 80 , the growth ratio between the LSS I and the welding area decreased. This phenomenon partially explains why LSS 2 cannot reach the bulk strength of the material mentioned above. Furthermore, it is also worth noting that, when measuring the welding area, the subjective judgment of the author to the fusion area will inevitably cause the errors of measurement of the actual welding area.

Table 2. Welded area of the joints with different flat energy directors

Thickness of FED	Weld melting area (mm^2) with different material of FED				
	No FED	Pure PP	1% EG/PP	3% MWNT/PP	20% SGF/PP
No FED	82.28±3.12	-	-	-	-
0.1 mm	-	81.75±8.32	117.64±4.68	66.31±3.34	102.31±3.57
0.2 mm	-	92.35±5.34	78.64±3.28	79.66±5.12	112.41±6.32
0.3 mm	-	74.25±4.21	97.41±4.37	36.75±6.14	79.34±5.13

3.3. The Effect of Thickness and Viscosity of Flat Energy Director on the Temperature of the Weld Interface

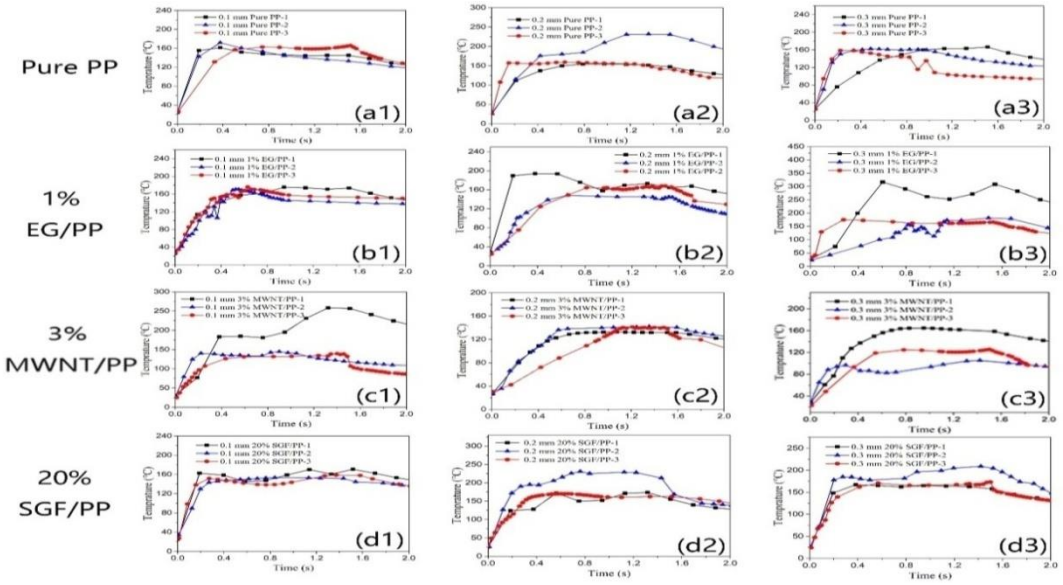

Figure. 6. Real-time temperature curves of the joints with different flat energy director (FED); a1-a3 for the joints welded with pure PP FED; b1-b2 for the joints welded with 1% EG/PP FED; c1-c2 for the joints welded with 3%MWNT/PP FED; d1-d2 for the joints welded with 20% SGF/PP.

The previous results prove that the thickness and viscosity of FED greatly influence the mechanical properties and welding area of the joints. In this part, the real-time temperature evolution at the welding interface was studied to better understand how flat energy directors (FED) affect the LSS of joints and interface, as shown in Fig. 6. In order to get the temperature on the interface, a temperature data collection system was used to measure the temperature on the

interface, as shown in Fig. 2b. It can be found from Fig. 6 that when the adherends of PP were welded with different FED, the heat could generate once the ultrasonic vibration was applied. At the initial stage of the welding process, the temperature at interface rose very quickly; most temperature curves leveled off at a temperature of about 160℃ after a time-lapse of about 0.4 s.

This temperature plateau coincides with the onset melting temperature (Tonset) of the FED as measured by DSC (shown in Fig.1c and d). The rapid temperature rise during the initial stage of the welding process is due to friction heating of the contacting surface (12,15). The measured temperature rate at the initial stage has been shown in figure 7a. It can be found in Fig. 7a that the initial rate of the increased temperature of the welding interface varied from 350 ℃-500 ℃, where the joints with a thickness of 0.1 mm FED had a higher temperature rate. In addition, the joints with Pure PP FED and 20% SGF/PP FED, where these two materials are quite different as to the viscosity, achieved a higher temperature rate at the initial welding stage. However, the joints welded with 0.2 mm and 0.3 mm 3% MWNT/PP FED, which has the same viscosity with 20% SGF/PP FED, achieved the lowest rate of temperature rise at the initial welding stage. The above analysis indicates that the thinner FED has an improvement to the initial temperature rate, and the effect of viscosity on the rate of temperature rise is complicated and dispersive.

After the initial welding process, the temperature reached a plateau for the most welding joints as shown in Fig. 6, which represented the material softens and flows along the entire bond line. However, there are two phenomena that are different from the ones reported in the paper (14,15,22): (1) ultrasonic welding characteristic stages are ambiguous and random for the most joints; (2) the temperature that leveled out was smaller than the melting temperature (Tpeak) of FED. These joints with different ultrasonic welding stages are more inclined to be influenced by the position of thermocouple, which itself acts as an energy director. The temperature of the joints at the welding time of 1s with different FED was shown in Fig. 7b. These results, shown in Fig. 7b, indicated that the middle area of the welding interface was not completely melted for most joints, which will be proved in the following section. The main reason for this problem is the size of the welding horn (as shown in Fig.2b) cannot concentrate the ultrasonic energy at the welding interface. This huge horn definitely causes a large part of the ultrasonic energy to be consumed in the form of mechanical waves into the air. It is worth pointing out that even the temperature curves with the same FED were scattered. Due to the contact temperature measurement of the thermocouple, this scattering is inevitable. Furthermore, note that these temperature data shown in Fig.6 are just the temperature of one point on different welding interfaces and cannot reflect the temperature of the entire welding interface. Of course, its existence also indicated that the above phenomenon exists on this welding interface, which is indelible and needed to make a good foundation for future research.

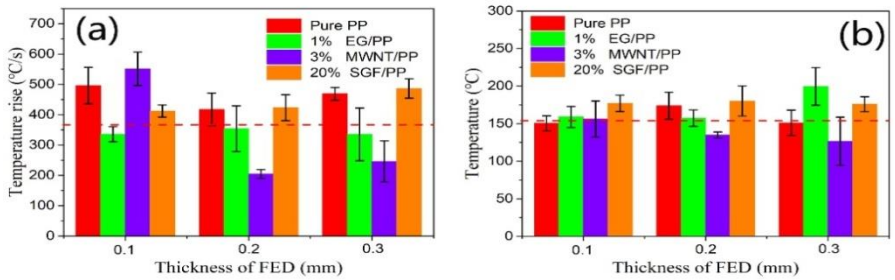

Figure 7. (a) The initial temperature rate of the joints welded with different FED, which stands for the average rate of temperature rise from the start to the first inflection point. (b) The temperature of the joints at the welding time of 1s with different FED. Note that the red dash line in Fig. 7a and b represent the initial temperature rate and temperature at the welding time of 1s of the joints without FED.

3.4. Welding Surface Observations

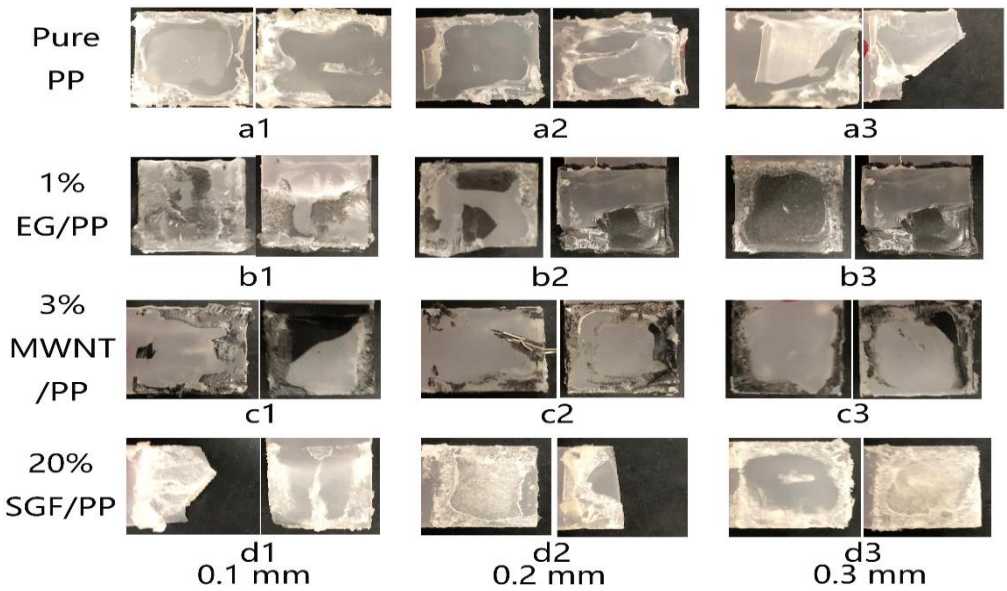

Fig. 8 Fracture surface of the joints with different flat energy director of the lap shear test. a1-a3 for the joints welded with pure PP FED; b1-b2 for the joints welded with 1% EG/PP FED; c1-c2 for the joints welded with 3%MWNT/PP FED; d1-d2 for the joints welded with 20% SGF/PP

Fig. 8 illustrates the fracture analysis of the joints with different flat energy directors after the lap shear test. As Fig.8 definitely shows, the melting and flow of matrix at the interface started at the edges of the overlap, while the middle area of the interface was intact and unmelted. This coincides with the temperature measurement results as shown in Fig. 7b. As far as the melting area is concerned, the melting area of the joints with 3%MWNT/PP FED is smallest, and the intermolecular fusion depth between adherend and FED is on the nanometer level. In addition, the melting area and morphology of the interfaces with 1% EG/PP FED and 20% SGF/PP are much bigger and coarse. For the joints with 1% EG/PP FED at a thickness of 0.1 mm, intermolecular fusion between adherend and FED happened in the middle area of the interface, which exactly explained its maximum lap shear strength shown in Fig.4a. One of the reasons that caused this phenomenon is the stiffness and volume of the thinner flat energy director (0.1 mm) at the interface are lower than that of the other FED (0.2 and 0.3 mm), its longitudinal deformation will be larger and the heat needed to melt will be less. For the joints with 20% SGF/PP FED that has the biggest viscosity among these four types of FED, almost no resin was squeezed out of the welding interface, which is conducive to creating beautifully welded joints. As shown in Fig. c2, the thermocouple indeed acted as an energy director, where much resin was melted around it. Whether the existence of thermocouple at the interface to the lap shear strength is harmful or not will be studied in the future, because of the importance of the temperature evolution for the development of ultrasonic welding technique.

In order to further understand the failure mechanism of the joints welded with flat energy director, the SEM details of the fracture surface were investigated (as shown in Fig. 8). It can be found in Fig. 8a that the obvious tearing streaks were observed, which indicated the intermolecular fusion has happened between adherent and FED and the interfacial bound was excellent. Thus, its fracture mechanism was a cohesive failure. In Fig. 8c, a lot of voids and the agglomerated carbon nanotubes (shown in red dotted circle) can be clearly observed and no tearing streaks (brittle fracture), which indicated that the intermolecular fusion only happened on the nanometer-level surface. Thus, its fracture mechanism was an adhesive failure. The

phenomenon that happened in the joints with 3%MWNT/PP FED was owning to the higher viscosity of FED, which caused many cavitation bubbles to be left trapped at the bond line at the end of welding [19]. The SEM details of the fracture surface of the joints with 20% SGF/PP FED was shown in Fig. 8d. In addition to the obvious tearing, streaks were observed, some glass fibers (millimeter level) were embedded in the interior of the adherend, and it formed a mechanical interlocking effect between adherend and FED, which was another major reason for its excellent strength. Thus, its fracture mechanism was a cohesive failure and a fiber-matrix debonding failure. Therefore, from the above analysis, the failure mechanism of the joints with flat energy director is a mixer of adhesive failure, cohesive failure, and fiber-matrix debonding failure..

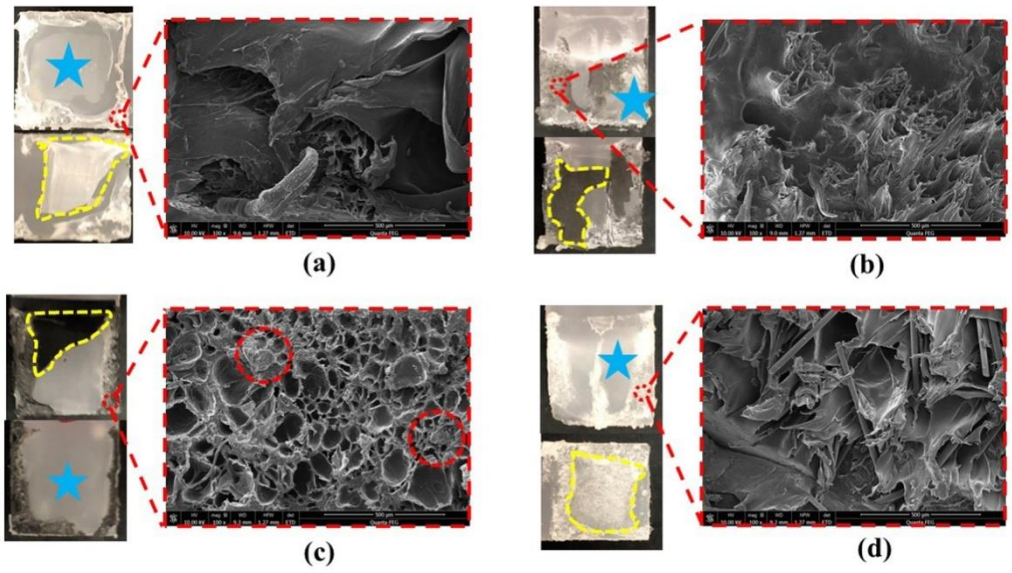

Fig. 8 Fracture surface (left) and SEM detail (red dotted box) for the joints welded with different flat energy director. The yellow dotted box represents the area of unmelted FED at the interface; the blue star represents the area of unmelted adherend at the interface. The red dotted circle represents the agglomerated carbon nanotubes.

A detail facture mechanism schematic diagram was shown in Fig. 9. The peeling stress toward the out-of-plane direction of the adherends occurred around the welding
area owing to a concentration of the tensile load. In addition, the in-plane tensile and compressive stresses were distributed around the edges of the welding area. The fracture of the joints initiated from the delamination and local buckling of the flat energy director owing to the out-of-plane peeling and in-plane compressive. As a result of the stress concentration at the free-edge sides shown in the red circle, the tensile strength of adherend will be weakened and less than the bulk strength. Sometimes it was broken before the welded interface was broken. Thus, these results that were illustrated above indicated that the lap shear strength Ⅱ will always be smaller than the tensile strength of the bulk material (adherend).

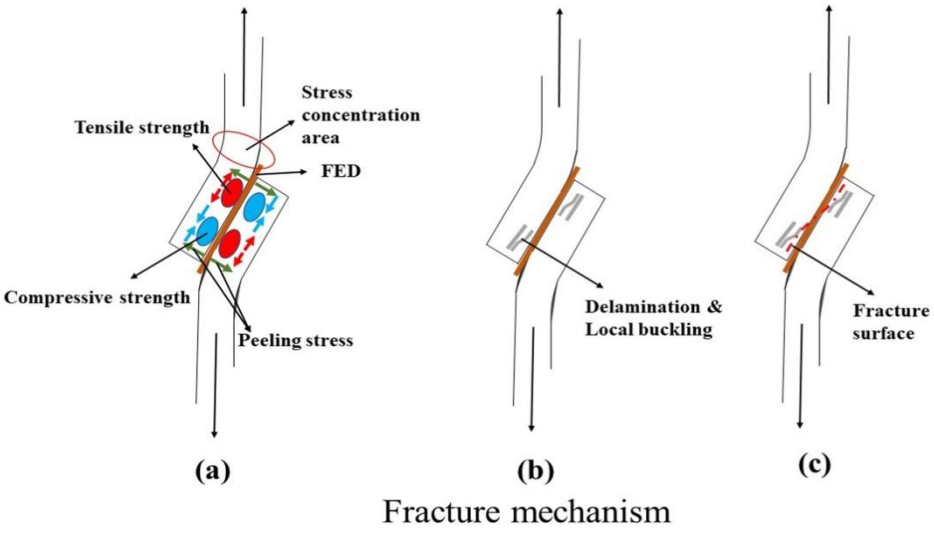

Fig. 9 Fracture mechanism of the joints with a flat energy director.

4. CONCLUSION

In this paper, the effect of the flat energy director on weld strength and stability was investigated. Specifically, the thickness and viscosity of FED on the weld quality. In the experiments, lap shear strength Ⅰ and lap shear strength Ⅱ that are the indicators for "welding efficiency" and "welding quality," respectively were measured to evaluate the weld quality. The actual welded area was obtained from fractured surface observations of the joints after the tests. To get a better understanding of the properties of flat energy director on the lap shear strength and the formation and failure mechanisms of the joints, the temperature evolutions at the interface were monitored and morphology analysis was carried out on the fracture surface. Based on the experimental results, a detail fracture mechanism was derived (shown in Fig. 9). The main conclusions of this paper are summarized as follows:

The mechanical tests showed that Lap shear strength (LSS Ⅰ) of the joints with FED welded at a thickness of 0.1 mm and 0.2 mm achieved a higher value. In addition, it can be found that at some specific thickness LSS Ⅰ of the joints added with these four different FED exceeded LSS I of the joints without FED. In particular, LSS Ⅰ of the joint added with 0.1 mm 1% EG/PP FED reached the highest value of 8.44 MPa, a 29.4% improvement over LSS I of the joints without FED. Comparing with the joints welded with pure pp, the LSS Ⅰ of the joints with 1% EG/PP FED, which has a viscosity of 3.18×106 mPa•s almost 1.3 times bigger than that of pure pp, is bigger than it under the condition of same FED thickness. However, LSS Ⅰ of the joints welded with 3% MWNT/PP FED, which has a viscosity of 4.28×106 mPa•s almost 1.7 times bigger than that of pure pp, is smaller than that of the joints with PP FED and without FED. Furthermore, the scatters of LSS Ⅰ for the joints with FED are less than that for the joints without FED. Thus, the use of FED with a thinner thickness (0.1-0.2 mm) and slightly higher viscosity had a great improvement on the weld strength and weld strength stability. Although the welding quality of the joints with FED appears to be larger than that of the joints without FED, the joint quality seems to be insufficient in comparison with a tensile strength of adherend, e.g 35 MPa.

It can be found that the welded area of the joints with 0.3 mm FED is lower than that of the joints welded with 0.1 mm and 0.2 mm FED, which has a good agreement with the LSS I. The welded area of the joint added with 0.1 mm 1% EG/PP FED reached the highest value of 117.64 mm2, a

42.97% improvement over the welded area of the joints without FED. Furthermore, there is a significant positive correlation between the lap shear strength Ⅰ (LSS Ⅰ) and the welded area of the joints added with FED. When the welding area was greater than 80 mm2, the growth ratio between the LSS Ⅰ and the welding area decreased.

The real-time temperature curves showed that, at the initial stage of the welding process, the temperature at interface rose up very quickly. Most temperature curves leveled off at a temperature of about 160 ℃ after a time-lapse of about 0.4 s. There are two phenomena that are different from the ones reported in the paper: (1) ultrasonic welding characteristic stages are ambiguous and random for the most joints; (2) the temperature that leveled out was smaller than the melting temperature (Tpeak) of FED.

Morphological analysis reveals that the melting and flow of matrix at the interface started at the edges of the overlap, while the middle area of the interface was intact and unmelted, which has a good agreement with the temperature measurement results. For the joints with 1% EG/PP FED at a thickness of 0.1 mm, the intermolecular fusion between adherend and FED happened in the middle area of the interface, which exactly explained its maximum lap shear strength. For the joints with 20% SGF/PP FED that has the biggest viscosity among these four types of FED, almost no resin was squeezed out of the welding interface, which is conducive to creating beautifully welded joints. The SEM details of the fracture surface showed that the intermolecular fusion and mechanical interlocking effect happened between adherend and FED, which indicated that the failure mechanisms of the joints with flat energy directors are a combination of adhesive failure, cohesive failure, and fiber-matrix debonding failure. Additionally, the fracture of the joints initiated from the delamination and local buckling of the flat energy director owing to the out-of-plane peeling and in-plane compressive.

There are certain limitations to this study. When measuring the LSS, the sample bars may break at the stress concentration area but not on the contacting area. When measuring the real-time temperature, the result obtained can only represent the temperature at one point but not the entire welding surface. Further optimization on ultrasonic welding can take consideration of the limitations.

This work would be helpful to understand the joint formation mechanism and the mode of failure by ultrasonic welding with the flat energy director and to optimize the welding process further.

ACKNOWLEDGMENT

This work was supported by the National Natural Science Foundation of China (Grant No. 51672201) and 2019 National College Student Innovation and Entrepreneurship Training Program Support Project (Project No. 201910497021).

REFERENCES

[1] Ishikawa T, Amaoka K, Masubuchi Y, Yamamoto T, Yamanaka A, Arai M, et al. Overview of automotive structural composites technology developments in Japan. Composites Science and Technology. 2018;155:221-46.

[2] Yousefpour A, Hojjati M, Immarigeon J-P. Fusion Bonding/Welding of Thermoplastic Composites. Journal of Thermoplastic Composite Materials. 2016;17(4):303-41.

[3] Shi H, Villegas IF, Bersee HEN. Strength and failure modes in resistance welded thermoplastic composite joints: Effect of fiber–matrix adhesion and fiber orientation. Composites Part A: Applied Science and Manufacturing. 2013;55:1-10.

[4] Villegas IF, van Moorleghem R. Ultrasonic welding of carbon/epoxy and carbon/PEEK composites through a PEI thermoplastic coupling layer. Composites Part A: Applied Science and Manufacturing. 2018;109:75-83.
[5] Zhao T, Palardy G, Villegas IF, Rans C, Martinez M, Benedictus R. Mechanical behaviour of thermoplastic composites spot-welded and mechanically fastened joints: A preliminary comparison. Composites Part B: Engineering. 2017;112:224-34.
[6] Suresh KS, Rani MR, Prakasan K, Rudramoorthy R. Modeling of temperature distribution in ultrasonic welding of thermoplastics for various joint designs. Journal of Materials Processing Technology. 2007;186(1-3):138-46.
[7] J LS, T CI, W HS. Factors affecting the joint strength of ultrasonically welded polypropylene composite. Polymer Composites. 2001;22(1):132-41.
[8] H P. Ultrasonic welding — Principles & theory. Materials and Design. 1984;5(5)::228-34
[9] Chan WX, Ng SH, Li KHH, Park W-T, Yoon Y-J. Micro-ultrasonic welding using thermoplastic-elastomeric composite film. Journal of Materials Processing Technology. 2016;236:183-8.
[10] Levy A, Le Corre S, Fernandez Villegas I. Modeling of the heating phenomena in ultrasonic welding of thermoplastic composites with flat energy directors. Journal of Materials Processing Technology. 2014;214(7):1361-71.
[11] Fernandez Villegas I, Valle Grande B, Bersee HEN, Benedictus R. A comparative evaluation between flat and traditional energy directors for ultrasonic welding of CF/PPS thermoplastic composites. Composite Interfaces. 2015;22(8):717-29.
[12] Villegas IF. Strength development versus process data in ultrasonic welding of thermoplastic composites with flat energy directors and its application to the definition of optimum processing parameters. Composites Part A: Applied Science and Manufacturing. 2014;65:27-37.
[13] Palardy G, Villegas IF. On the effect of flat energy directors thickness on heat generation during ultrasonic welding of thermoplastic composites. Composite Interfaces. 2016;24(2):203-14.
[14] N T, H NT, T WR. Ultrasonic welding using tie-layer materials. part I: Analysis of process operation. Polymer Engineering and Science. 1992;32(9):600-11.
[15] Tao W, Su X, Wang H, Zhang Z, Li H, Chen J. Influence mechanism of welding time and energy director to the thermoplastic composite joints by ultrasonic welding. Journal of Manufacturing Processes. 2019;37:196-202.
[16] Levy A, Le Corre S, Poitou A. Ultrasonic welding of thermoplastic composites: a numerical analysis at the mesoscopic scale relating processing parameters, flow of polymer and quality of adhesion. International Journal of Material Forming. 2012;7(1):39-51.
[17] Gleich DM, Van Tooren MJL, Beukers A. Analysis and evaluation of bondline thickness effects on failure load in adhesively bonded structures. Journal of Adhesion Science and Technology. 2001;15(9):1091-101.
[18] Hopmann C, van Aaken A. Ultrasonic welding of polyamide—influence of moisture on the process relevant material properties. Welding in the World. 2014;58(6):787-93.
[19] G R, H NT, T WR. Ultrasonic welding using tie‐ayer materials. part II: Factors affecting the lap‐hear strength of ultrasonic welds. Polymer Engineering and Science. 1992;32(9):612-9.
[20] Goto K, Imai K, Arai M, Ishikawa T. Shear and tensile joint strengths of carbon fiber-reinforced thermoplastics using ultrasonic welding. Composites Part A: Applied Science and Manufacturing. 2019;116:126-37.
[21] Villegas IF, Bersee HEN. Ultrasonic welding of advanced thermoplastic composites: An investigation on energy-directing surfaces. Advances in Polymer Technology. 2010;29(2):112-21.
[22] Zongbo Z, Xiaodong W, Yi L, Zhenqiang Z, Liding W. Study on Heating Process of Ultrasonic Welding for Thermoplastics. Journal of Thermoplastic Composite Materials. 2009;23(5):647-64.